Article:

2

3   **Public domain satellite gravity inversion offshore Somalia combining layered-Earth and**

4   **voxel based modelling**

5   Gaud Pouliquen[1]*, Gerry Connard[2], Hannah Kearns[3], Mohamed Gouiza[4] and Douglas Paton[4]

6   Geosoft Europe, Oxford, UK | [2] Geosoft US, Corvallis, US | [3] Spectrum Geo | [4] Leeds University * Corresponding author, E-
7   mail: gaud.pouliquen@geosoft.com

8

9   **Introduction**

10   At the end of 2016, Spectrum Geo released two long offset seismic reflection profiles across the Somalian rifted margin, in the
11   Juba Lamu and Obbia basins respectively – part of two larger 2D surveys acquired in 2014 and 2015/16 (Stanca et al., 2016;
12   Figure 1). In frontier areas, potential field data interpretation, in particular public domain satellite-derived gravity, can play a
13   key role in the early stages of exploration by identifying basement structure, sediment thickness, and the continental-oceanic
14   crust transition (COT) or continental-oceanic boundary (COB), and hence indirectly contribute to the understanding of thermal
15   history and the hydrocarbon system. This is particularly relevant over the Somalia margin, where geophysical surveys have been
16   extremely sparse until very recent years.

17   A high-gradient in the gravity is often used as a marker of the COB along passive margins (see Pawlowski (2008) for a
18   review), expressing laterally contrasting physical properties between the continental and oceanic crusts. However, at magma-
19   poor rifted margins, such as the Somalia margin, the lithosphere undergoes a progressive thinning/stretching process and the
20   transition between unaltered continental crust and oceanic crust becomes gradual (Manatschal, 2004). Crustal hyper-extension,
21   serpentinization, embrittlement, and exhumation of mantle peridotites can precede accretion of true oceanic crust, which in
22   turn can blur the simple transitional model between a dense and highly magnetized oceanic crust and a weakly magnetized
23   and lighter continental crust. Along a magma-poor margin, analysis of potential field data can distinguish the different rifting
24   domains and quantify crustal thinning (Stanton et al., 2016; Cowie et al., 2015). In offshore Kenya and Somalia, the image is
25   further complicated by thick sedimentary cover.

26   To overcome this complexity, we attempt here to map both the basement structure and the density distribution over the
27   margin through a combined, or hybrid, modelling approach. We adopt a co-operative inversion approach where the results of
28   a conventional layered-earth based structural inversion are fed into a voxel-based inversion to produce a final 3D distribution
29   of density variation over the Obbia basin. This 3D approach is supported by a series of regional 2D gravity models along the

30   margin. With the exception of shipborne bathymetry, the study was conducted using public domain data, the satellite derived
31   gravity data (Sandwell et al., 2014), and focused on the offshore areas: data onshore were only included to maintain the regional
32   character of the model.

33   We built on the experience gained from a previous voxel-based inversion of the vertical gravity gradient G_{zz} over a well-
34   known area of the Gulf of Mexico (MacLeod et al., 2016), which showed that a relatively simple inversion scheme of public
35   domain gravity could lead to a realistic 3D model of the subsurface.

36   Our models reveal partitioned and variable basement architecture and sediment distribution from south to north along the
37   Somalia margin. It also reveals areas of hyper-extended crust and possible exhumed mantle in the Obbia basin, as suggested
38   by Stanca et al. (2016).

39   This study demonstrates that meaningful results can be drawn from a relatively simple inversion scheme, relying on public
40   domain data. This type of approach is a valuable, low-cost aid for mapping the density of the earth in frontier areas, and to
41   facilitate basin exploration. The approach also has scope for application in better-understood basins.

42   **Data and methodology**

43   The area presented in this study is a large area offshore East Africa, geologically complex and sparsely surveyed, located between
44   -/+8˚ latitude and encompassing the Western Somalian Basin and part of the Northern Somalian basin (Figure 1). While our

45 main objective is to better understand the crustal architecture over the margin, a second objective of our work was to evaluate
46 the added value of a combined inversion scheme. This type of modelling is sometimes referred to as hybrid, and has been mostly
47 applied for sub-salt exploration (Ellis et al., 2015). Conventional gravity 3D inversion for hydrocarbon exploration relies mostly
48 on a layered-earth approach, where the inversion returns discrete interfaces, while assuming a constant density within each layer.
49 It makes for an intuitive modelling process and often suffices to recover the crystalline basement geometry. It is also fast since
50 most available algorithms work in the frequency domain. However, assuming a constant density can be misleading in areas of
51 greater complexity.

52 To map any density variations from the initial regional model (green polygon on Figure 1), we follow up the structural
53 inversion using Geosoft's GM-SYS 3D program with a voxel-based inversion over a smaller area (black polygon on
54 Figure 1), using Geosoft's VOXI Earth Modelling inversion (Geosoft Inc., 2017).

55 One of the challenges in combining voxel and layered models in a hybrid inversion is that voxel inversions generally
56 produce models which have 'smoothed' transitions between domains whereas layered earth models have discrete transitions.
57 To overcome this inconsistency, a series of constraints can be set up during the voxel inversion to ensure that we honour the
58 layered nature of the physical properties distribution. Finally, a last challenge for the VOXI inversion can be the size of the
59 model as even with high-performance computing, it remains comparatively significantly slower than a frequency domain
60 inversion. The area in the study covers nearly $2.9 \cdot 10^6$ km^2, and we opted for a trade-off between computation time and
61 resolution by running the density inversion over the Obbia basin only, where the seismic data revealed more complexity.

62 We used the Free-Air satellite derived gravity anomaly (FAA; Sandwell et al., 2014; 2 mgal accuracy), and work with G_z,
63 rather than the vertical derivative G_{zz}, as we did in the Gulf of Mexico, since we want to image density variations within the
64 sediment and the upper crust.

65 We first built an initial 3D regional density volume from global crustal models, and used published refraction data to
66 constrain sediment densities. The initial Moho depth is from the Crust 1.0 model (Laske et al., 2013). For the initial sediment
67 thickness, we used the recent NOAA global sediment thickness map (Whittaker et al., 2013). Shipborne bathymetry data were
68 provided by Spectrum Geo over the seismic survey area (H. Kearns, personal communication), and completed with the
69 Sandwell bathymetry offshore (Sandwell and Smith, 1997), and the SRTM data onshore. When using satellite gravity, such a
70 modelling approach is enhanced if the bathymetry measurements are independent from the gravity, and the final model is more
71 reliable where there are bathymetric soundings.

72 From the three DSDP holes in the area (DSDP 234, 235 and 241; Figure 1), only DSDP 235, located east of Chain Ridge,
73 reached acoustic basement and recovered basalts with a density of 2.9 gcm^{-3}.

74 In the 2D and 3D starting models, the densities of the basement rocks are assumed constant: 3.3 gcm^{-3} for the mantle, 2.9
75 gcm^{-3} for the lower continental and oceanic crust, 2.7 gcm^{-3} for the upper continental crust and 2.75 gcm^{-3} for the upper oceanic
76 crust. For the sediments, we derived densities from refraction data located in the south west corner of our model, offshore
77 Kenya (Makris et al., 2012), using a Nafe-Drake density depth function to convert from V_p to densities.

78 In parallel, we also built a series of long regional gravity 2D models from south to north along the margin. Two of the
79 models over the Juba Lamu and Obbia basins integrate Spectrum Geo published seismic data, and help in calibrating our
80 regional 3D model. A starting top lower crust surface was created by extrapolating the 2D models and using half the
81 thickness of the crystalline crust in areas distant from the model. The Moho, top lower crust and top basement surfaces were
82 then successively inverted within GM-SYS 3D to fit the observed FAA. This layered-Earth model is imported as a density
83 volume into VOXI to calculate a residual Gz anomaly (bathymetry-lower crust-Moho reduced), which is in turn inverted
84 with a set of constraints to recover a 3D distribution of density variations. The full workflow is summa-rized below.

85 Modelling sequence:

86 • We upward continue Gz to 1 km above Mean Sea Level.

87 • We built 2D gravity models, using seismic when available. A top lower crust horizon is added to each of these
88 models.

89 • We built a layer-based 3D density model of the subsurface, including seafloor, top basement, top lower crust and
90 Moho, using Geosoft GM-SYS 3D. We used a density-depth function derived from the Makris et al. (2012) model for the
91 sediments. This al-lows a rapid calculation of the model's gravity anomaly in the frequency domain.

92 • We successively invert the Moho, top lower crust and top basement horizons to fit the long wavelength of the
93 FAA. The final model is exported as density volume.

94 •   We calculate a residual gravity anomaly, corrected from the bathymetry, lower crust and Moho contributions and
95 invert it in VOXI to recover a volume of density variations.

96 We add these variations to the starting density model to obtain a final density model over the area.

2D gravity modelling

98 We carried out six long regional gravity models along the margin. We present three models from south to north (Figures 2-4).
99 For the Juba Lamu and Obbia basins, we integrated the two time-migrated, 15 s TWT seismic sections published by Stanca et
100 al. (2016). Although the reflection profiles are shorter than our models, which extend beyond the margin itself, they provide
101 valuable ties for the model main horizons.

102 Stanca et al. (2016) describes a change in crustal architecture from south to north, with the continental-oceanic transition
103 progressing farther seaward, which is confirmed by our models.

104 In Juba Lamu (Figure 2), the geophysical signature of the COB is unambiguous. The lateral changes in seismic character and
105 gravity anomaly allow for clear identification of the oceanic crust. The FAA displays a steep gradient approximately 180 km
106 from the present coastline, which is modelled by a relatively rapid transition from a stretched continental crust to a 7-9 km thick
107 oceanic crust and a contrast of 0.5 gcm^{-3} in density within the upper crust. Version 2 of the World Digital Magnetic Anomaly
108 Map (WDMAM; Lesur et al., 2016) and extinct ridges identified by Phethean et al. (2016) over this portion of the Western
109 Somali basin support the location of the COB.

110 The proximal margin over the Juba Lamu basin displays a low gravity, and the 2D models required the addition of diapiric
111 structures, with a density of 2.2 gcm^{-3} to fit the observed anomaly. Interpreted initially as Jurassic salt diapirs by Coffin and
112 Rabinowitz (1987), more recent interpretation of modern seismic data suggests that these structures are more likely to be
113 gravitational shale diapirs (H. Kearns, personal communication). The density in our model is consistent with measured
114 densities for shale diapirs, reported between 2.1-2.3 gcm^{-3} (Graue, 2000).

115 Farther north in the Coriole basin (Figure 3), although the transition between continental and oceanic crust remains easily
116 identifiable in our model. We locate the COB 215 km from the actual coastline, suggesting a wider zone of
117 transitional/stretched continental crust and enhanced thinning of the continental crust. The signature of the COB is partly
118 attenuated by a thicker sedimentary cover, ~ 4.9 km thick.

119 In the Obbia basin (Figure 4 a,b), bounded in the North by the Auxiliary Rescue and Salvage Fracture Zone (ARS FZ),
120 separated from the Coriole basin in the south by a pronounced bathymetric high at 4∘N, both Spectrum Geo seismic and the
121 gravity models suggest that we enter a different and more complex rift domain. Here, the necking zone is wider (120 km),
122 followed by hyper-extended crust and possibly exhumed mantle (Stanca et al., 2016; Figure 4a,b). The COB is not readily
123 apparent. Farther seaward along the profile (Figure 4a), i.e. beyond the hyper-extended crust domain, the interpretation is
124 farther complicated by an area of uplifted basement (Figure 4b) exhibiting late or post-rift tectonic activity, and characterized
125 by a gravity high and a magnetic high (based on WDMAM map).

126 Stanca et al. (2016) discussed alternative gravity models and interpretations for the Obbia basin. In one model, a zone of stretched
127 crust, is followed by exhumed mantle (with a density of 3.2 gcm^{-3}) juxtaposing oceanic crust east of the ARS FZ, i.e. east of the
128 basement high. In a second model, the high is interpreted as a volcanic high with a uniform density of 2.9 gcm^{-3}. Mantle
129 exhumation is accompanied by serpentinization of peridotites. Densities are strongly negatively correlated with the degree of
130 serpentinization and highly variable, going from 3.3 gcm^{-3} for 0% serpentinization, down to 2.5 gcm^{-3} for 100% (Miller and
131 Christensen, 1997). Hence, without further constraint, a range of densities is possible to model serpentinized mantle. Our
132 simplest model (Figure 4a,b) suggests that a hyper-extended upper/lower crust (<3 km thick) with unchanged 2.7/2.9 gcm^{-3}
133 densities fits the observed FAA adequately. Substituting this two-layer model by a single layer of stretched crust at 2.9 gcm^{-3} also
134 provides an acceptable fit. However, introducing an exhumed mantle at 3.2 gcm^{-3} largely overestimated the FAA (by more than 30
135 mgal) and is not viable. Most recent interpretations of magma-poor passive margins argue in favour of the presence of exhumed
136 serpentinized mantle, and Cowie et al. (2015) have found on the Iberian-Newfoundland margin that the extremely thinned crust (<3
137 km) suggests the presence of an exhumed mantle. Serpentinization has also been suggested to vary rapidly with depth, with the first
138 2 km being more highly serpentinized. Although speculative, a hyperextended crust, followed by exhumed mantle at 2.7/2.9 gcm^{-3}
139 seems to be a plausible interpretation of both the seismic and gravity data. Farther oceanward the nature of the basement high
140 remains to be constrained: again a simple two-layer model with 2.75/2.9 gcm^{-3} densities suffices to fit the observed FAA. But signs
141 of late/ post rift tectonic activity could argue in favour of a tectonic high formed of exhumed mantle with a higher serpentinization
142 rate in the upper first few kilometres, and consequently lower density than for the serpentinized mantle described earlier in the
143 northwest of the basin. The adjacent long reflection line located north of the model, where tilted continental blocks are present,
144 could support this hypothesis (Mohamed Gouiza, personal communication). In all scenarios, oceanic crust is not present closer
145 than 350 km from the actual coastline (Figure 4a).

Layered-earth-based gravity modelling and structural inversion

The initial regional density model (Figure 1) integrates an initial COB derived from Coffin and Rabinowitz (1987), significantly modified in the north based on the 2D gravity models and the magnetic data (EMAG2 v3, Meyer et al., 2017). We chose a 0.5 gcm^{-3} density contrast between the upper continental and oceanic crusts. For the sediments, we extrapolate the 1D density-depth function derived from the Makris et al. (2012) refraction line.

Once this initial model is compiled, we then run successive structural inversions within GM-SYS 3D. We start with the deepest interface, the Moho, and then the top lower crust and then the top crystalline basement, with the aim of fitting the longer wavelengths of the observed G_z. We use the Bouguer onshoreFree-Air offshore of the Sandwell v23 satellite derived gravity with a 2.67 gcm^{-3} Bouguer reduction density.

Since the voxel inversion intends to recover density variation within the sediments and the upper crust, we residualize the observed FAA from deeper contributions and produce a reasonable starting density model for the inversion. After the structural inversion, 95% of the error between the observed and calculated G_z ranges between ± 8 mgal (Figure 5), with a standard deviation of 11 mgal. The misfit increases in areas where we had fewer constraints: onshore Africa and Seychelles, as well as in the southwest corner of the grid, with little effect on the offshore model.

The crustal thickness and sediment isochore maps after inversion (Figures 6 and 7) highlight the partitioning of the margin into three distinct areas from north to south, which encompass the Juba Lamu, Coriole and Obbia basins and the heterogeneous sediment distribution along the margin, with thicker sediment cover in the Juba Lamu basin. In the Obbia basin, the isochore map after inversion shows significant thinning on the eastern, deep part of the basin, located beyond the seismic survey (Figure 7), where a gravity high is observed.

The most notable change in crustal thickness in our model occurs in the north of the margin, north of the VLCC ridge and over the Obbia basin. The combination of the NOAA data and Crust 1.0 Moho indicates a large area of stretched continental crust east of the ARS FZ and oceanic crust between the ARS FZ and the Chain Ridge. Our model proposes an area of highly thinned crust east of the ARS FZ in the Obbia basin (< 5 km thick). This thinned crust also extends north of the ARS FZ.

Voxel-based gravity inversion over the Obbia basin

Once the regional Moho, top lower crust and top basement surfaces are adjusted, we then export a voxelized density model from GM-SYS 3D for a smaller area covering the Obbia basin. We worked with a mesh of 2000 m x 2000 m horizontally and 100 m vertically (Figure 8), rapidly increasing downward at the depth of ~5400 m (deepest bathymetric point) ending up with a model that contains 23 million cells. In VOXI, the bathymetry is accurately represented by using a Cartesian Cut Cell method (Ellis and McLeod, 2013). This allows us to calculate a precise terrain model using a density contrast of 0.77 gcm^{-3} between the youngest sediments and the water. Because we aim to recover density variations from our starting model, within the sediments and the upper crust, we first calculate the contribution of the bathymetry, mantle and lower crust, and subtract them from the observed FAA. This residual anomaly is VOXI's input (standard deviation of 5 mGal).

VOXI allows constrained inversions, both spatially and in terms of physical property range. This means that available geological and geophysical data, such as a density-depth function inferred from wells, or seismically constrained basement depth, can be easily integrated to guide the inversion through a series of constraints. For the inversion over Obbia, we apply several constraints to take into account the inherent characteristics of the physical property distribution within the study area:

1. Starting model and parameter reference models: both are set as our initial density model for the sediment and the upper crust, and to a null density from the top lower crust downward since we have removed the contribution of deeper layers (Figure 8).

2. Density upper and lower bounds: we expect densities to vary within a realistic range, so we bound the densities between 1.8-2.7 gcm^{-3} in the sediments and 2.6-2.9 gcm^{-3} in the upper crust.

3. We introduce a differential gradient weighting between the NS/EW gradients and the vertical gradient, set to 10 and 0.1 respectively.

We apply two passes of the iterative reweighting process (IRI; Ellis, 2012) that emphasizes positive and/or negative properties.

The inversion algorithm then seeks to minimize the misfit between the response of the starting model and the input residual anomaly, and returns a 3D volume of density variations. To interpret the final model, we can extract horizontal slices parallel to a reference surface at regular intervals. In Figure 9, we compare density slices between the starting and final models taken from the top of the lower crust upward at 1000 m intervals.

Discussion

Based on the joint analysis of the gravity anomalies, density inversion results, along with the crustal thickness, sediment isochore and 2D gravity models, we sketch three different domains, A, B and C, corresponding to three distinct crustal domains within the study area (Figure 10).

Domain A corresponds to the proximal margin, a north-south corridor, approximately 120 km wide, and is associated with the necking zone. Here our 3D starting density model has been left fairly untouched by the VOXI inversion (Figure 9) and the range of densities is in good agreement with the 2D model.

Domain B encompasses the distal margin and is the most complex area. Combining density slices and crustal thickness below 5km, we outline an area of hyperextended crust, coherent with t he section identified by Stanca et al. (2016), and our 2D model along Spectrum Geo line (Obbia model, Figure 4a). The area shows several pockets of density reaching 2.9 gcm^{-3}. Some of these can be interpreted as exhumed mantle, and this is likely to be the case in the area of gravity high marked by a star on Figure 10. Without any further structural constraint on its nature, we left out the tectonic high identified on Spectrum Geo profile (Figure 4a) located at the intersection of the ARS FZ and the seismic profile. Domain C is a SW-NE trending V-shaped oceanward domain, located in deep water (~ 5 km deep), starting in the northeast of the area, bounded by Chain Ridge to the east, and dying against the ARS FZ to the south. This area is characterized by a thick sediment cover and thin crust. The calculated first vertical derivative of the FAA, G_{zz}, and the Tilt derivative also reveal a series of distinctive lineaments, oriented at 10° NW, and display a distinct corrugated or grainy texture, gradually disappearing toward the south. Neither the EMAG2 v3 data nor the latest version of the WDMAM magnetic grids give enough clues of the nature of the magnetic anomaly, and no clear magnetic stripes are present on the west side of Chain Ridge. At the southern tip of this area we had identified potential oceanic crust along both the seismic and 2D model (i.e. southeast of the tectonic high). The crust there is adjacent to unambiguous oceanic crust on the opposite side of Chain Ridge. Both the calculated densities in the upper crust leaning toward 2.9 gcm$_{-3}$, and the crustal thickness could suggest an affinity with oceanic crust. However, without unequivocal recorded oceanic magnetic anomalies, we can only speculate on its nature.

Conclusions

The combination of 2D and constrained-combined 3D modelling has revealed rifted domains along the Somalian margin defined by distinct basement architectures and density distribution. In the north of the margin over the Obbia basin and in the area beyond in the Northern Somalian basin, the density model indicates more complexity than farther south, and potential extensive areas of hyperextended crust. The model argues in favour of Cochran's (1988) early suggestion that the area west of the ARS FZ and north of 4°N may be extended continental crust, although we would extend this domain north of the ARS FZ. The model has also confirmed an oceanward progression of oceanic accretion, lying at ~180 km from the coastline in the Juba Lamu basin, 215 km in Coriole and ~350 km in Obbia.

Today's high performance computing makes possible large-scale regional satellite gravity inversion and this study reveals how public domain data inversion can provide a realistic density model of the subsurface and help us to understand frontier domains. Though these approaches are particularly interesting in frontier basins with little or no seismic coverage, we argue that there is perhaps even an application for better-understood basins where existing seismic data and wells are used to build more rigorous constraints into the inversion.

Acknowledgments

References

Cochran, J.R. [1988]. Somali Basin, Chain Ridge, and origin of the Northern Somali Basin gravity and geoid low. Journal of Geophysical Research: Solid Earth, **93**, 11985-12008.

Coffin, M.F. and Rabinowitz, P.D. [1987]. Reconstruction of Madagascar and Africa: Evidence From the Davie Fracture Zone and Western Somali Basin, Journal of Geophysical Research, **92**, 9385-9406.

241 Cowie, L., Kusznir, N. and Manatschal, G. [2015]. Determining the COB location along the Iberian margin and Galicia Bank from
242   gravity anomaly inversion, residual depth anomaly and subsidence analysis. Geophysical Journal International, **203.2**, 1355-1372.

243 Ellis, R.G. [2012]. Iterative Reweighted Inversion. Geosoft Technical Note, http://www.geosoft.com/products/voxiearth-
244   modelling/iterative-reweighting-inversion.

245 Ellis R.G. and MacLeod, I.N. [2013]. Constrained voxel inversion using the cartesian cut cell method. 23rd Geophysical Conference,
246   Extended Abstracts.

247 Ellis, R., Connard G., Popowski, T. and Pouliquen, G. [2015]. Hybrid strategies for modelling gravity gradient data. International
248   Work- shop and Gravity, Electrical & Magnetic Methods and their Applications. Expanded Abstracts.

249 Graue, K. [2000]. Mud volcanoes in deepwater Nigeria. Marine and Petroleum Geology, **17.8**, 959-974.

250 Laske, G., Masters., G., Ma, Z. and Pasyanos, M. [2013]. Update on CRUST1.0 - A 1-degree Global Model of Earth's Crust. Geophys.
251   Res. Abstracts, **15**, EGU2013-2658.

252 Lesur, V., Hamoudi, M., Choi, Y., Dyment, J. and Thébault, E. [2016]. Building the second version of the World Digital Magnetic Anomaly
253   Map (WDMAM). Earth, Planets and Space, **68** (1), 27.

254 MacLeod, I.N., Connard, G. and Johnson, A. [2016]. Inversion of Public Domain Gravity Gradient Data in the Gulf of Mexico. 78th EAGE
255   Conference and Exhibition 2016-Workshops, Extended Abstracts.

256 Makris, J., Papoulia, J., McPherson, S. and Warner, L. [2012]. Mapping of sediments and crust offshore Kenya, east Africa: a wide aperture
257   refraction/reflection survey. 2012 SEG Annual Meeting, Expanded Abstracts.

258 Manatschal, G. [2004]. New models for evolution of magma-poor rifted margins based on a review of data and concepts from West Iberia
259   and the Alps. International Journal of Earth Sciences, **93**, 432–466.

260 Meyer, B., Saltus, R. and Chulliat, A. [2017]. EMAG2: Earth Magnetic Anomaly Grid (2-arc-minute resolution) Version 3. National Centers for
261   Environmental Information, NOAA. Model.

262 Miller, D.J. and Christensen, N.I. [1997]. Seismic velocities of lower crustal and upper mantle rocks from the slow-spreading Mid-Atlantic Ridge,
263   south of the Kane Transform Zone (MARK). In: Karson, J.A., Cannat, M., Miller, D.J., and Elthon, D. (Eds.), Proc. ODP, Sci. Results, **153,**
264   College Station, TX (Ocean Drilling Program), 437–454.

265 Pawlowski, R. [2008]. The use of gravity anomaly data for offshore continental margin demarcation. The Leading Edge, **27** (6), 722-727.

266 Phethean, J.J.J., Kalnins, L.M., van Hunen, J., Biffi, P.G., Davies, R.J. and McCaffrey, K.J.W. [2016]. Madagascar's escape from Africa:
267   A high-resolution plate reconstruction for the Western Somali Basin and implications for supercontinent dispersal. Geochem. Geophys.
268   Geosyst., **17**, 5036–5055.

269 Sandwell, D.T., Muller, R.D., Smith, W.H.F., Garcia, E. and Francis, R. [2014]. New global marine gravity model from CryoSat-2 and
270   Jason-1 reveals buried tectonic structure. Science, **346**, 65-67.

271 Smith, W.H. and Sandwell, D.T. [1997].. Global sea floor topography from satellite altimetry and ship depth soundings. Science, **277**
272   (5334), 1956-1962.

273 Stanton, N., Manatschal, G., Autin, J., Sauter, D., Maia, M. and Viana, A. [2016]. Geophysical fingerprints of hyper-extended, exhumed
274   and embryonic oceanic domains: the example from the Iberia–Newfoundland rifted margins. Marine Geophysical researches, **37** (3),
275   185-205.

276 Stanca, R., Kearns, H., Paton, D., Hodgson, N., Rodriguez, K. and Hussein, A.A. 2016, Offshore Somalia: crustal structure and implications
277   on thermal maturity. First Break, **34** (12), 61–67.

278 Whittaker, J.M., Goncharov A., Williams S., Müller R.D. and Leitchenkov, G., [2013]. Global sediment thickness dataset updated for the
279   Australian-Antarctic Southern Ocean, Geochemistry, Geophysics, Geosystems, **14** (8), 3297-3305.

280 VOXI, Geosoft Inc. [2017]. http://www.geosoft.com/products/ voxi-earth-modelling/overview, accessed on 25 July 2017.

281

282

283
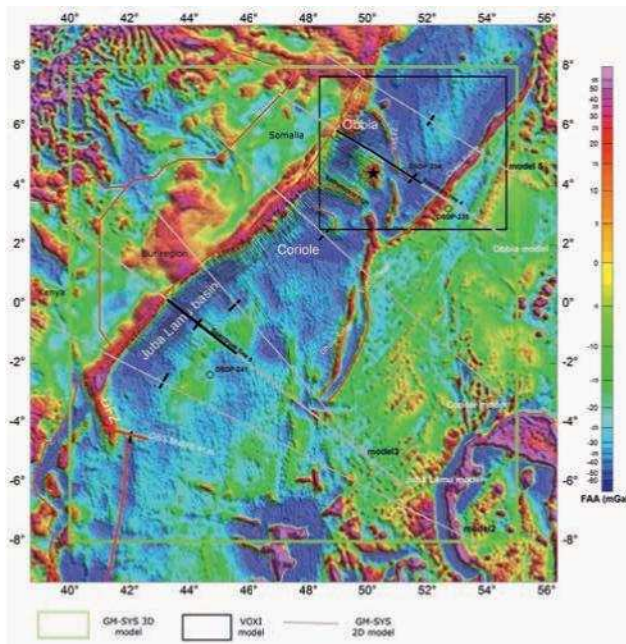
Figure 1 Map showing the satellite derived Free Air gravity anomaly G_z (shaded with calculated G_{zz}). The green polygon indicates the extent of the layered-Earth 3D model (GM-SYS 3D model), the grey lines show the location of the 2D gravity models (the COB/COT location on each model is indicated by a thick black line). The black polygon shows the extent of the VOXI density inversion. In the south, the red EW line shows the OBS profile used for velocity-density conversion (Makris et al., 2012). Red lineaments indicate basement ridges and fracture zones (Davie Fracture Zone (DFZ), Very Large Crude Carrier (VLCC), Dhow Ridge and Chain Ridge. Spectrum survey tracks indicated by thin black lines. The black star indicates possible exhumed mantle (Stanca et al., 2016).

289
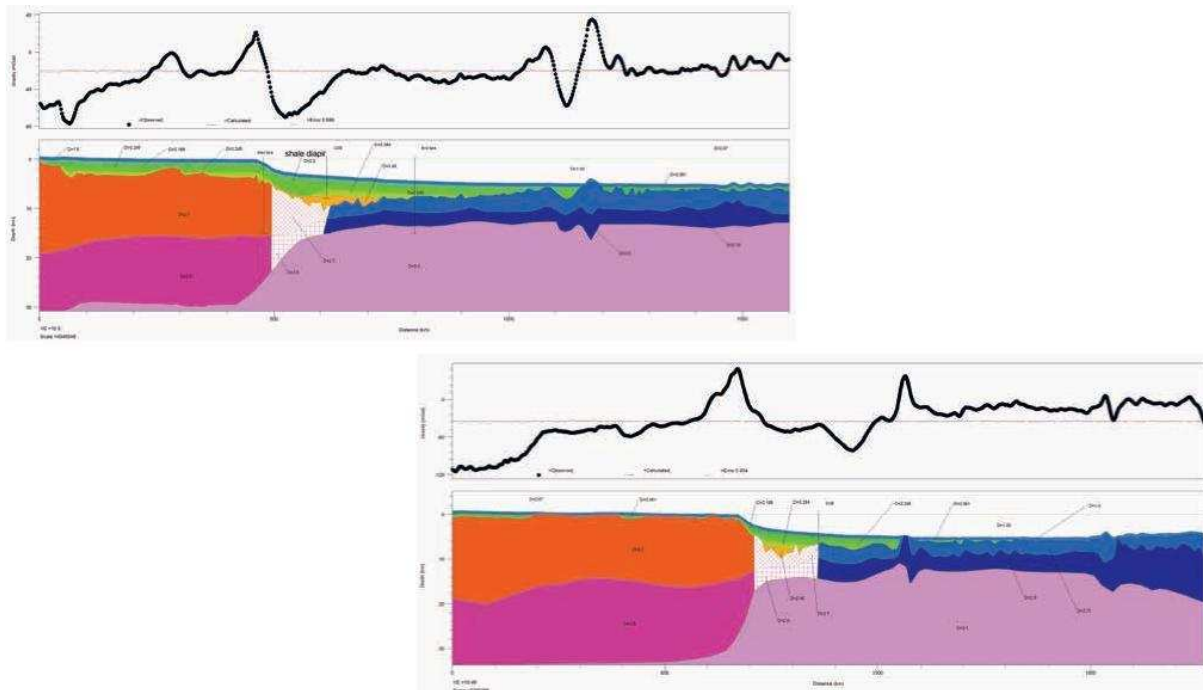
Figure 2 Juba Lamu gravity model (see location on Figure 1). Vertical lines indicate the start and end points of the Spectrum Geo seismic along the profile. The interpreted COB is also indicated by a thin vertical line. Transitional/stretched continental crust is indicated by hatch patterns blocks in the model.

292
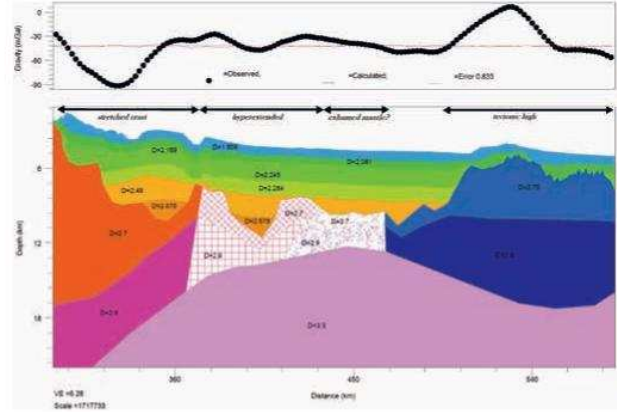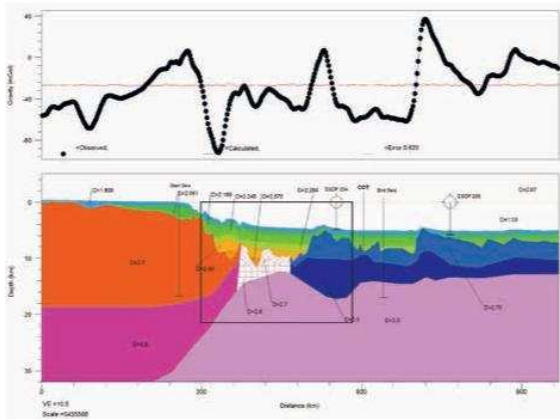
Figure 4 a) Obbia gravity model. The start and end points of the corresponding seismic profile are indicated by thin vertical lines. The black polygon shows the zoomed area in Figure 4b. Interpreted COT is indicated by a black vertical line. b) Zoom of the gravity model of the rifted margin in Obbia Basin, Figure 4a.
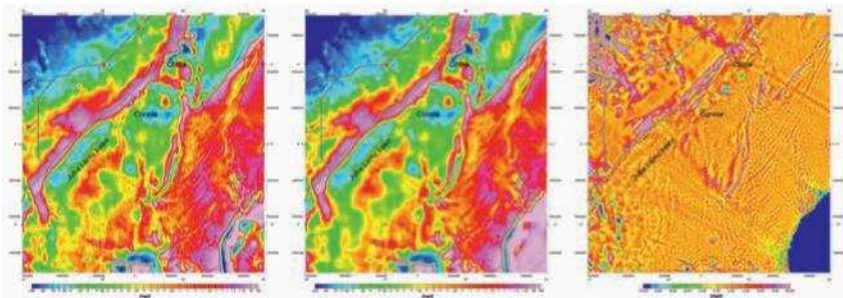
295

Figure 5 From left to right: observed Bouguer-FAA, calculated anomaly, and error map in mGal. The observed and calculated grids are displayed with the same colour scale using histogram equalization. The error grid is displayed with a linear distribution.
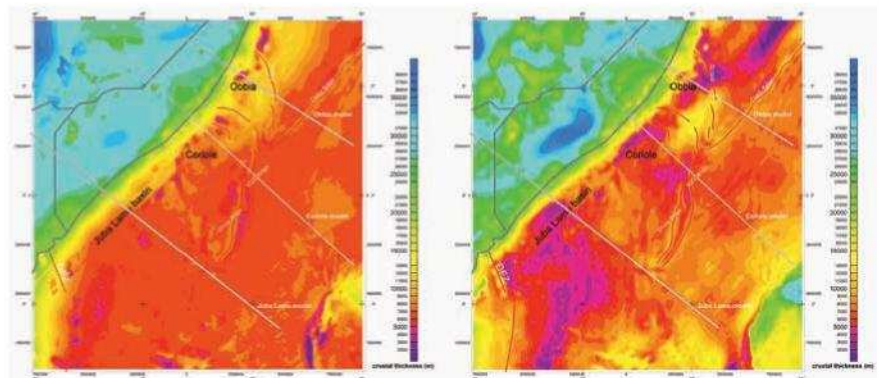

Figure 6 crustal thickness map before (left) and after inversion (right), displayed using a linear scale. Grey lines show the location of the 2D models.
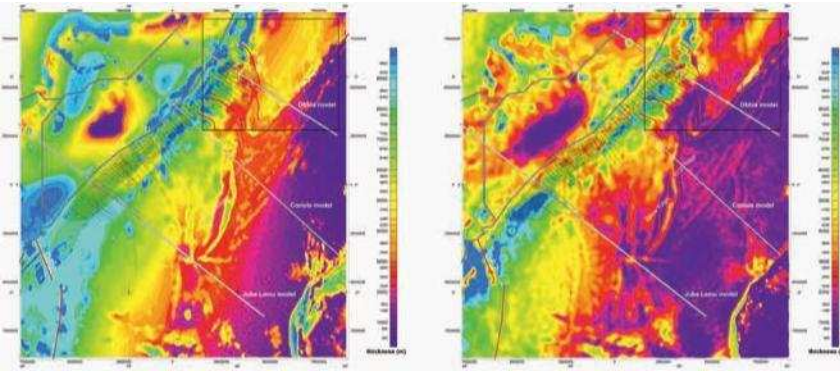
296
297
298
299
300
301
302
303
304

Figure 7 Sediment isochore maps before (left) and after inversion (right) displayed with a linear distribution. Cold colours indicate thick sediments while hot colours show thin sediments. Spectrum Geo survey shown in black. Black polygon shows the Obbia area for VOXI inversion.
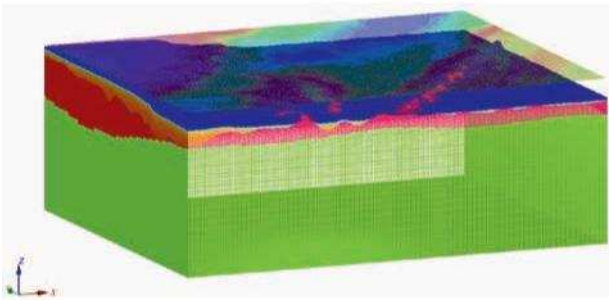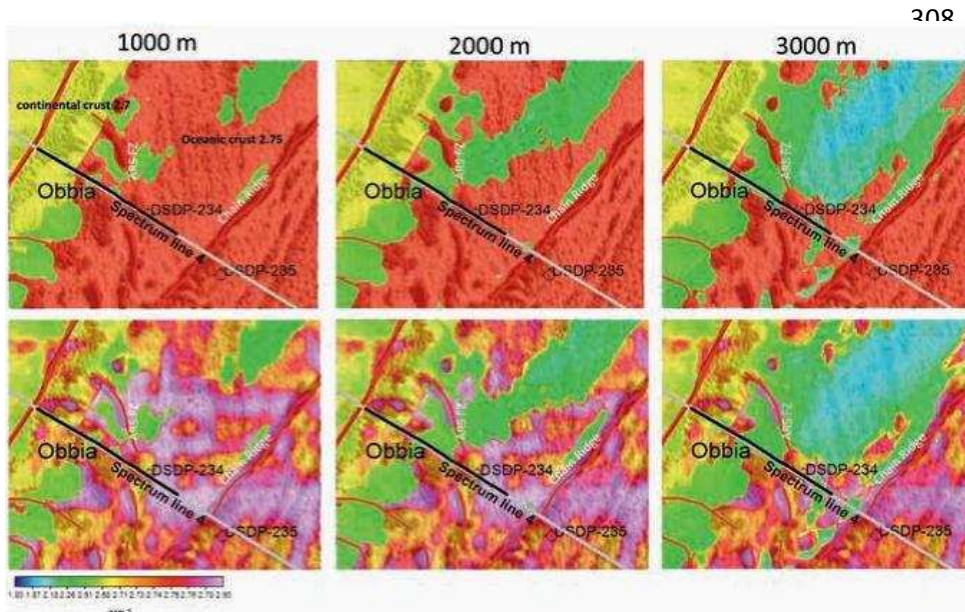

305
306
307

Figure 8 Orthographic view of VOXI mesh and starting model showing density distribution within the sediments and the upper crust. Vertical cell size increases downward. Density is set to zero below the top lower crust (green volume). The overlay grid shows the residual G_z.

308

321
322
323

Figure 9 Density slices at 1000 m intervals upward from the top lower crust before (top) and after VOXI inversion (bottom). All grids are displayed with the same colour scale. The grey line indicates the 2D gravity model while the black line shows the extent of Spectrum Geo seismic data. The density is shaded with the calculated first vertical derivative G_{zz}

324
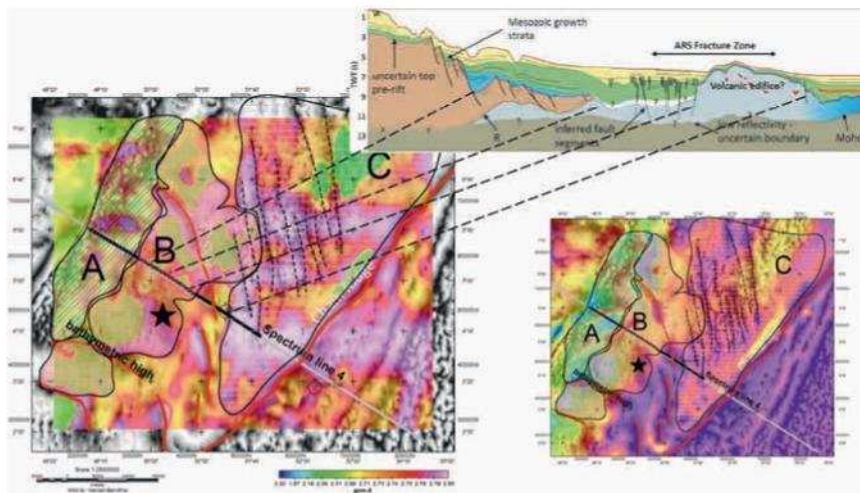
Figure 10 Schematic interpretation into crustal domains A,B,C. The main map on the left displays modelled densities as a slice 1000 m above the lower crust surface, overlaid on the grid of the tilt derivative of G_z (grey colour scale). Basement ridges and bathymetric highs are outlined in red. The black star shows possible exhumed mantle. NW-SE dashed lines correspond to lineaments picked on the tilt derivative. Top right: Spectrum Geo TWT seismic line, as modelled in Figure 4a (from Stanca et al., 2016). Bottom right: sediment isochore map overlaid on G_z tilt derivative (the sediment isochore grid is displayed with same colour scale than used on Figure 7